



Ambient vibration testing, dynamic identification and model updating of a historic tower

Dora Foti^{a,*}, Mariella Diaferio^a, Nicola Ivan Giannoccaro^b, Michele Mongelli^a

^a Dipartimento di Ingegneria Civile e Ambientale, Politecnico di Bari, 70126 Bari, Italy

^b Dipartimento di Ingegneria dell'Innovazione, Università del Salento, 73100 Lecce, Italy

ARTICLE INFO

Article history:

Received 28 July 2011

Received in revised form

28 November 2011

Accepted 30 November 2011

Available online 29 December 2011

Keywords:

Historical buildings

Ambient vibration test

Operational modal analysis

FE model identification

Model updating

ABSTRACT

The results of an ambient-vibration based investigation conducted on a historical tower in Italy, to update the 3-D finite element model of the building are presented in this work. The main difficulties are related to the extreme **in-homogeneity** of the building and the presence of an elevator vain that occupies the posterior part of the tower, forcing to locate the accelerometers only on one façade of the building.

The assessment procedure include **full-scale ambient vibration testing**, **modal identification** from ambient vibration responses using three different identification methods, finite element modeling and dynamic-based identification of the uncertain structural parameters of the model. **A very good match between theoretical and experimental modal parameters was reached and the model updating has been performed to identify some structural parameters.**

© 2011 Elsevier Ltd. All rights reserved.

1. Introduction

The study described in this paper was performed in order to evaluate the structural condition of the tower of the Provincial Administration Building in Bari, Italy, with the final purpose to predict the performance of the tower to different combinations of static and dynamic loads, for instance earthquakes or other induced vibrations.

In the last years, this field has attracted the interest of many researchers. In particular, ambient vibration testing has become the main experimental method available for assessing the dynamic behavior of full-scale structures [1] because no excitation equipment is needed, involving a minimum interference with the normal use of the structure. The procedure showed to be especially suitable for flexible systems, such as civic towers [2], bell-towers [3–6], masonries [7] and minarets [8].

One main problem in the Operational Modal Analysis (OMA) is the maintenance of the data acquisition system [9]. Field measurements, in fact, are often performed in very harsh environmental conditions, requiring high accuracy both in the control of the test set-up and in the analysis of the measured data. Moreover, measurements are usually noisy for the necessity of using very long cable transducers. Other relevant and common problems in the field of OMA are [10]: the difficulty to detect different mode shapes for very closely spaced modes; the subjectivity in the

system order estimate; the need of a more efficient algorithm able to omit the spurious modes created by noise or redundant degrees of freedom of the model.

Ambient vibration test has been conducted on the above mentioned tower, in a particularly windy day (24th July 2009), with the aim of determining its dynamic response and developing a procedure for modeling the tower. The Operation Modal Analysis (OMA) has been carried out both in the frequency domain and in the time domain to extract the dominant frequencies and mode shapes. The application of well-known different identification techniques—the Enhanced Frequency Domain Decomposition (EFDD) method [11], the Stochastic Subspace Identification (SSI) method [12] and the Crystal-Clear Stochastic Subspace Identification (CC-SSI) method [13]—implemented in a commercial software, yields to very similar results for all the identified modes, providing consistent information for the following finite element model updating.

The final goal of this research is to develop a 3D finite element model able to match the results of OMA. With this purpose, some uncertain parameters of the model (basically the Young's modulus and density of the cyclopic concrete masonry in different regions of the structure and some added masses, introduced to take into account the weight of non-structural elements) will be selected as “updating parameters” and iteratively modified to minimize the differences in the natural frequencies between FEM and OMA.

The obtained results are very good with an excellent match between the experimental data and the updated model, referred to the first five frequencies and their corresponding mode shapes.

* Corresponding author. Tel.: +39 080 5963771; fax: +39 080 5963719.
E-mail address: d.foti@poliba.it (D. Foti).

The details of the updating procedure will be shown in the following.

2. Description of the building

The tower of the Provincial Administration Building in Bari, Italy (Fig. 1), dating back to the thirties of the 20th century and



Fig. 1. View of the Provincial Administration Building of Bari with the investigated tower.

about 60 m tall, is not only a typical example of the fascist architectural style, but it is an important symbol of the city itself.

Situated on the waterfront of the city, with the principal façade exposed to the North–West direction (that is the dominant wind direction), the tower has eleven floors, characterized by different interstory heights and a square plan. In detail, the square plane has a side of about 9.0 m from the base to the 5th floor, a side of about 8.6 m from the 5th to the 9th floor, a side of about 7.6 m at the 10th floor, and a side of about 5.3 m at the 11th floor. It is made of massive concrete reinforced with a diffuse and superficial reinforcement and it stands on a foundation slab. The eleven levels of the tower consist of a basement, a mezzanine and nine floors. Up to the 5th floor, the tower is surrounded by the main part of the building of the provincial administration, from which it emerges for other six levels, from the 6th to the 11th ones, with openings on the façades in the first floor up to the building of the provincial administration and in the upper two floors, the last of which (the bell chamber) has a smaller plan with respect to the others.

The tower was instrumented with thirteen SA-107LNC uniaxial servo-accelerometers, (force-balance technology, specific for use in seismic and low level–low frequency motion studies, range ± 0.1 g, ± 2 g), placed at floors 5, 7, 9 and 10 and connected to a centralized data acquisition board by means of long transducer cables (Fig. 2). The details of the acquisition and the starting calibration are shown in [13]. The accelerometer position along the height of the tower, referred to the xyz reference system is shown in Fig. 3(a) while the quoted sections of the instrumented tower floors are shown in Fig. 3(b).

During the data elaboration, it was found that accelerometers indicated with 301 and 307 in Fig. 3(b) (floor 7 and 9) were out-of-order because their measurements were very noisy and no peak appears in their acceleration time–history plots when subjected to an impact with a hammer.

In Fig. 4 the typical acceleration time–histories recorded by the accelerometers 301 and 307 have been compared to the ones recorded by the accelerometers 304 and 296. The inspection of Fig. 4 reveals a remarkable difference between the time series, conceivably related to the different signal-to-noise (S/N) ratio of the four sensors.

As a consequence, the data recorded from sensors 301 and 307 have been neglected from the analysis, i.e. these accelerometers will not be considered in the present study.

As it is possible to notice from Fig. 3(a), all the accelerometers were placed along the same side of the tower. This choice derived from the difficulty of placing at the same level other

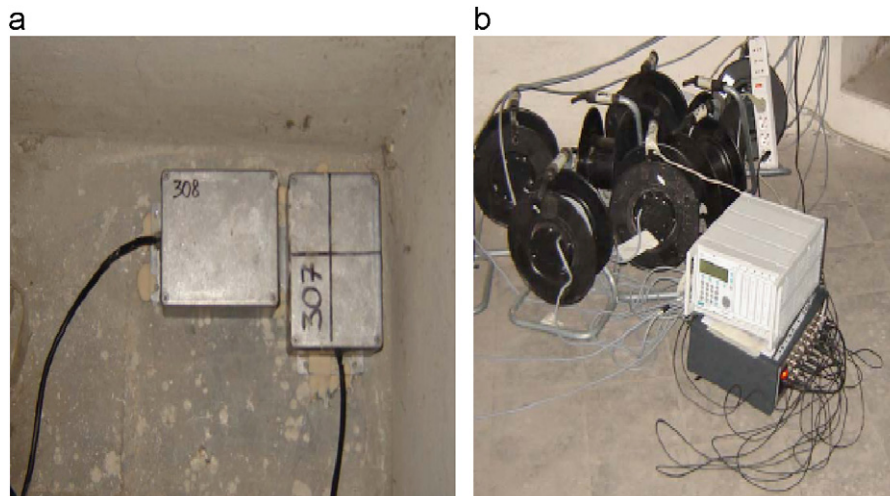


Fig. 2. Equipment used for the tests: (a) uniaxial accelerometers; (b) data acquisition board.

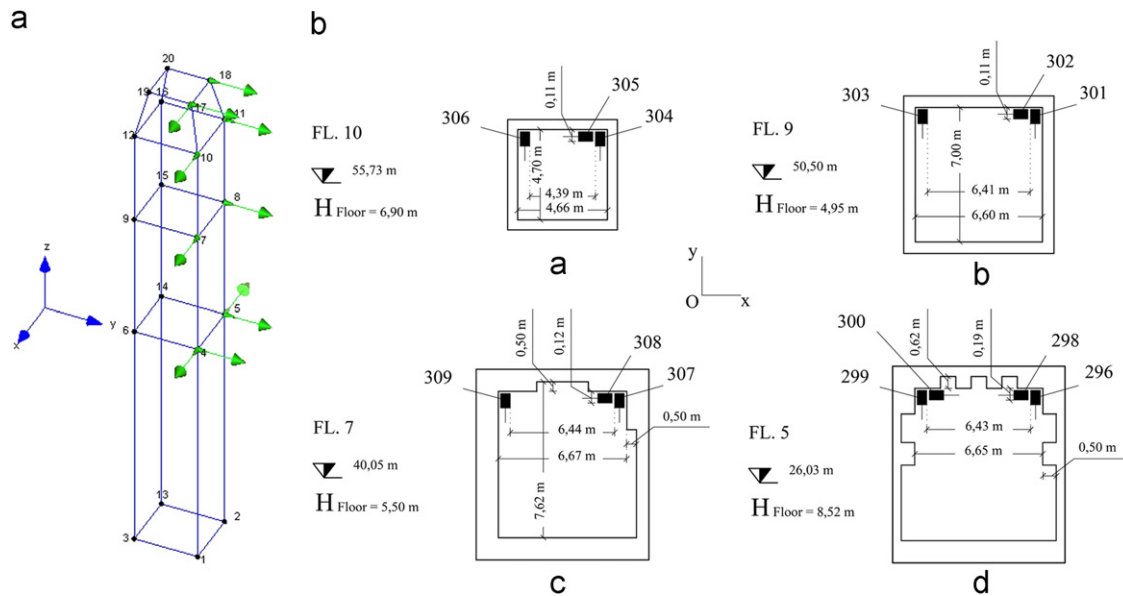


Fig. 3. Localization of the accelerometers: (a) on the tower using a model of 20 points (4 points for each instrumented plane); (b) quoted sections of the instrumented floors.

accelerometers at the opposite side of the building. One side of the internal part of the tower, in fact, was occupied by a steel staircase and a lift vain used to get to the terrace.

The ambient vibrations were registered in a particularly windy day (24th July 2009), during a time interval of 220 min, at a sample rate of 200 Hz. The idea was to perform a statistical analysis on the repeatability of the identified modal parameters. Considering that a time of 20 min is the minimum suggested for each acquisition, the total time interval of 220 min could permit to analyze eleven consecutive intervals. The choice of 11 intervals is related to the possibility of analyzing the stability and repeatability of the results and of guaranteeing the absence of harmonic casual excitations.

The signal conversion and the data acquisition were managed using a laptop in the framework of the CATMANv4 software package, which included an analogical filter with cut-off frequency of 40 Hz.

3. Data processing and operational modal analysis

On the basis of the results of [13], a new analysis was carried out. The analysis of the recorded data was carried out through a statistical analysis in order to evaluate the repeatability of the identified frequencies in the different intervals and, above all, the effects of the external disturbances. The frequencies identification was carried out considering the consistency of the identified frequencies on the eleven different intervals referred to consecutive time periods. The extraction of the modal parameters from ambient vibration data was carried out using the ARTEMIS software [14]. Three different OMA methods were used: EFDD, SSI and CC-SSI. Fig. 5(a)–(c) show the experimental results with reference to one of the eleven intervals considered. All the results were obtained with the maximum resolution allowed (8192 lines of spectral density).

Table 1 shows a synoptic table of the average values and the standard deviation of the first five estimated frequencies evaluated considering all the eleven time intervals and the three examined methods. In particular, Fig. 6 shows the average values of the first two frequencies and the graphs obtained considering the identified values of the first two frequencies for each method

and for each time interval, identified by a number from 1 to 11. Examining Fig. 6 and Table 1, it is possible to notice that the first two frequencies values are quite close, due to the symmetry of the tower section; moreover the three methods give similar results and there is a good consistency of the selected frequencies for all the considered time intervals with a very low standard deviation.

The observed mode shapes can be improved by introducing some relations between the measured and unmeasured degrees of freedom. In the framework of the ARTEMIS Extractor Pro software [14] it is possible to define linear combinations of the measured signals (the so-called “Slave Nodes Equations”) which can be very helpful for defining rigid body motions and slave nodes relations. These equations can be used to evaluate the vibrations of the instrumented points, and, as a consequence, to construct the mode shapes for the entire tower, even though the acquisitions are available only in few nodes of the geometry. In particular, the data have been analyzed imposing that each floor of the tower is rigid in its plane. In this hypothesis, in fact, the movement of each floor can be described imposing mathematical equations between the nodes coordinates in the xy plane [14]. In particular, considering the nodes classification shown in Fig. 3, equations were applied between the nodes groups (4,5,6,14), (7,8,9,15), (10,11,12,16) and (17,18,19,20). The modes depicted in Fig. 7 and in Table 1, may be classified as bending modes as the first (y-direction), the second (x-direction), the fourth (y-direction) and the fifth (y-direction), and torsional mode (the third one). The last one, nevertheless has been classified as a torsional mode, is not perfectly depicted, probably due to the low number of sensors used for each floor and their position on it; in fact this position is able to monitor the bending modes, but is surely inaccurate for the complete and correct reconstruction of the torsional modes. This choice, however, was obliged by the impossibility of placing any accelerometer on the opposite side of the tower for the presence of an internal elevator vain and a stair-case.

4. FE modeling

The experimental investigation was accompanied by the development of a 3D finite element model (Fig. 8) based on the

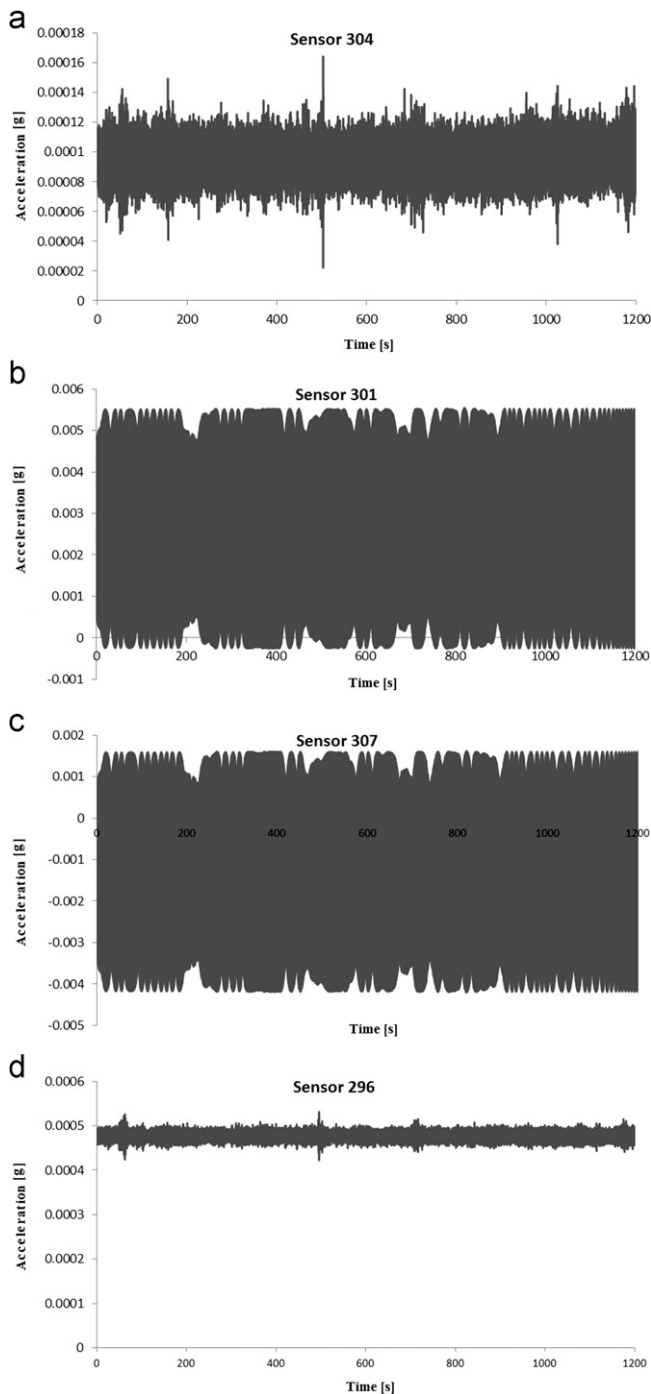


Fig. 4. Comparison between the acceleration time-histories recorded by sensors at different test point of the tower: (a) floor 10; (b) floor 9; (c) floor 7 and (d) floor 5.

geometrical survey, by means of the software SAP2000 [15] v.12 running on a processor Intel(R) Pentium(R) 4 CPU 3.00 GHz with a computing time around 27 min.

The tower was modeled using 8-node brick elements while the floors were represented by 4-node shell elements. The model has a total of 11,410 nodes, 4,923 solid elements (utilized to model the walls), 3,271 shell elements (utilized to model the floors). In formulating the model the following assumptions were adopted:

- The Poisson's ratio was held constant and equal to 0.2;
- Some springs (totally 30) were added for taking into account the interaction between the tower and the building of the

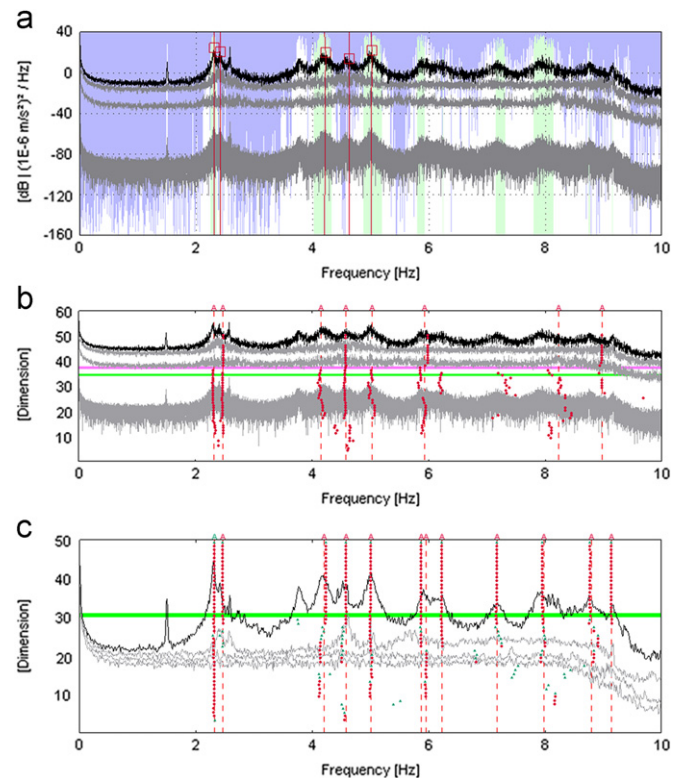


Fig. 5. Singular values of spectral density matrices by EFDD technique for interval number 10 (a), Stabilization diagram of the state space model by SSI technique for interval number 10. (b) and Stabilization diagram of the state space model by CC-SSI technique for interval number 10 (c).

Table 1

First five natural frequencies identified from ambient vibration measurements.

	EFDD [Hz]	St.Dev [%]	SSI [Hz]	St. Dev [%]	CC-SSI [Hz]	St. Dev [%]	Mean of the methods [Hz]
Mode 1	2.303	0.0033	2.303	0.0046	2.298	0.0106	2.301
Mode 2	2.398	0.0211	2.438	0.0291	2.440	0.0256	2.425
Mode 3	4.178	0.0164	4.172	0.0481	4.160	0.0588	4.171
Mode 4	4.594	0.0394	4.594	0.0308	4.593	0.0376	4.594
Mode 5	5.011	0.0197	5.021	0.0115	5.022	0.0178	5.017

provincial administration that surrounded the tower for the first five floors; some of these springs (20) are oriented along the x axis, the remaining 10 springs are oriented along the y axis. The springs have been introduced to describe the stiffness of the provincial administration building along the principal directions in plane for each floor; thus the springs have been concentrated at the corners of the tower in correspondence of each of the first five floors.

- Some masses (totally 44 non structural elements) were added at the corners of each floor to take into account the masses of the non structural elements.
- As indicated in similar examples in literature [4], usually the distribution of the Young's modulus and the spring constants are the structural parameters affected by major uncertainties. In this case, due to the presence of an elevator, that is inserted in the posterior part of the tower, and to the high in-homogeneity of the cyclopic concrete, that is the material that composes the walls of the tower, it has been established that the density and the Young's modulus could be associated to 11 different parts in which the tower is divided (Fig. 9), each one associated with one of the tower floors.

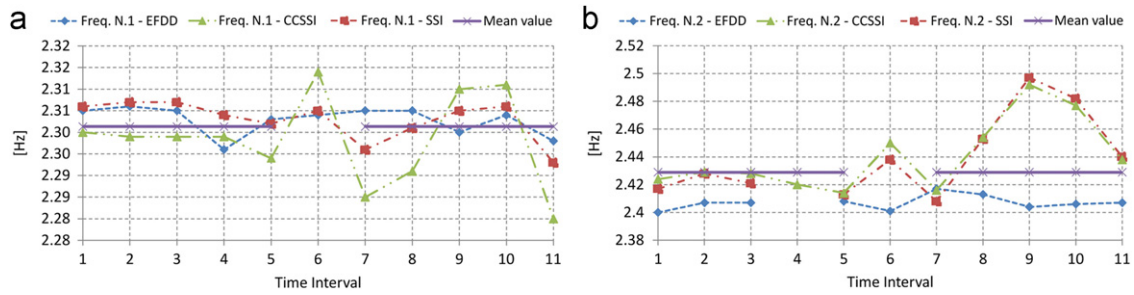


Fig. 6. Statistical analysis of the first two frequencies estimation.

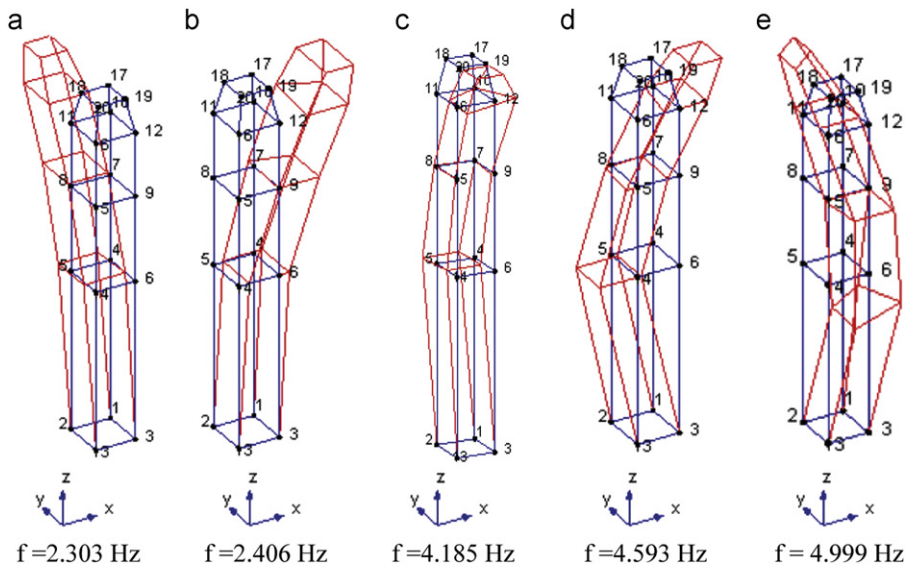


Fig. 7. Vibration modes identified from ambient vibration measurement.

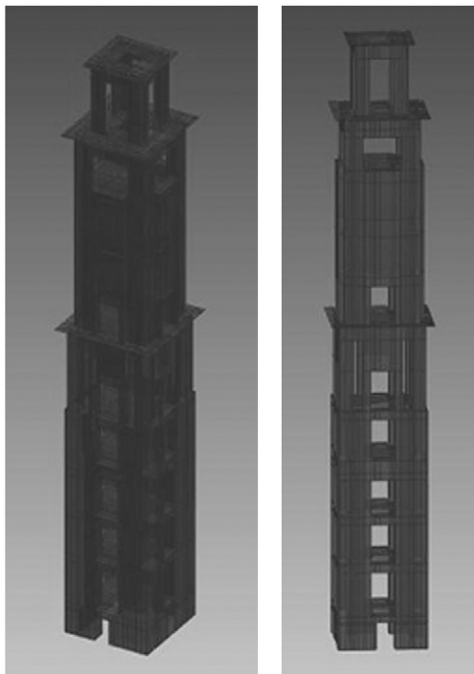


Fig. 8. Finite element modeling of the tower: (a) 3D view; (b) front elevation view.

5. Model updating procedure

The parameters selected for the updating procedure are the Young's modulus E_i and the densities ρ_i in the 11 zones indicated in Fig. 9; 30 springs (some along x -direction, some along y -direction) and 44 masses, that is 96 parameters were totally considered for the updating procedure.

Observing that an important part of the updating procedure, which may guarantee to achieve good results is strictly based on the good choice of the parameters starting values, it has been conducted an accurate analysis to evaluate their reasonable initial values. In detail the starting value for the Young's modulus (equal to 2.2×10^{11} N/m²) was estimated [16] as the average value obtained by two specimens extracted from internal walls at different floors of the tower (Fig. 10); the density was estimated testing in laboratory the aforementioned specimens of cyclopic concrete (starting value for all the zones equal to 2200 kg/m³). Moreover the added masses were obtained considering the masses associated to the non-structural elements evaluated assuming the dimensions as quoted in a technical report compiled several years ago for a retrofitting intervention; the initial values of the springs were estimated on the basis of the dimensions of the building.

A preliminary sensitivity analysis was carried on the 96 parameters; in Fig. 11 the normalized sensitivities of the vector of 96 parameters composed by 11 Young's modulus E_i , 11

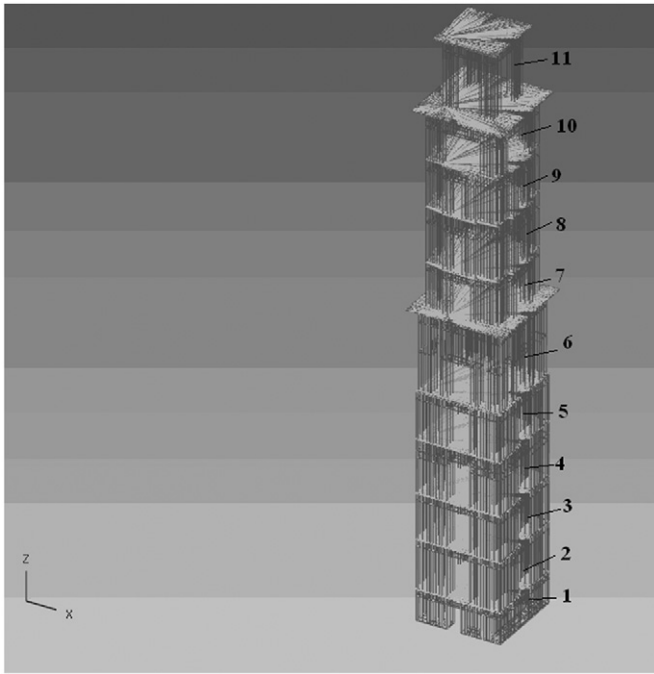


Fig. 9. Division of the FE model in 11 zones.

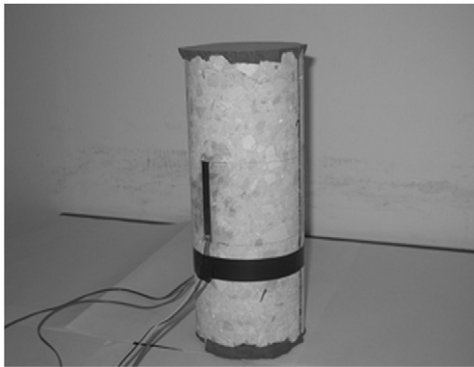


Fig. 10. Core sampling test of the cyclopic concrete.

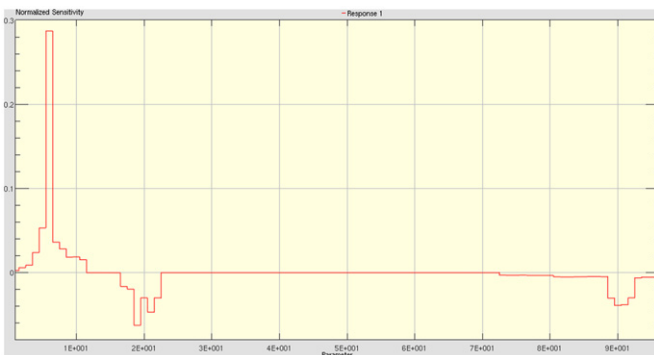


Fig. 11. Normalized sensitivity of the 96 parameters preliminarily considered for the updating.

densities ρ_i , 30 springs and 44 masses. It is possible to note that the sensitivity of the 30 springs is very low compared to the other parameters, so they were not used in the following model updating and totally 66 parameters were updated.

The method used for the normal modes evaluation in the 3D finite element model is the Lanczos subspace method [17], while the parameters estimation was carried out minimizing the differences between theoretical and experimental natural frequencies. It must be underlined that the updating procedure is referred to the frequencies because there is a good confidence on the identification of these parameters.

The strategy used for updating the 66 parameters previously indicated is the well-known Inverse Eigen-Sensitivity [18]. In detail [17]:

$$\mathbf{R}_e = \mathbf{R}_a + \mathbf{S} \cdot (\mathbf{P}_u - \mathbf{P}_0) \quad (1)$$

or in a short form:

$$\Delta \mathbf{R} = \mathbf{S} \cdot \Delta \mathbf{P} \quad (2)$$

where in (1): \mathbf{R}_e is the vector of the reference system responses (experimental data); \mathbf{R}_a is the vector of the predicted system responses for a given state \mathbf{P}_0 of the parameter values; \mathbf{P}_u is the vector of the updated parameter values; \mathbf{S} is the sensitivity matrix;

$$\Delta \mathbf{R} = \mathbf{R}_e - \mathbf{R}_a$$

$$\Delta \mathbf{P} = \mathbf{P}_u - \mathbf{P}_0.$$

Eq. (1) is usually underdetermined and can be solved using a pseudo-inverse (least squares) method, weighted least squares or Bayesian technique, depending on whether weighting coefficients are added or not. Since the Taylor's expansion is truncated after the first term, the neglected higher order terms necessitate several iterations, especially when $\Delta \mathbf{R}$ contains large values [19]. The applied least squares solution [19] will minimize iteratively the residue defined as:

$$residue = \mathbf{S} \cdot [\Delta \mathbf{P}_{n+1} - \Delta \mathbf{R}] \quad (3)$$

with $\Delta \mathbf{P}_{n+1}$ calculated as follows:

$$\Delta \mathbf{P}_{n+1} = [\mathbf{S}^T \cdot (\mathbf{S}^T \cdot \mathbf{S})^{-1}] \cdot \Delta \mathbf{R} \quad (4)$$

The previous procedure was applied to achieve the fixed convergence in a limited number of iterations, limiting the variation range of all the 66 parameters considered to the 50% of the starting value.

6. Comparison between experimental data and updated FE model

The comparison of the experimental data with the updated FE model is shown in Table 2 in which the first five estimated experimental frequencies, the first five frequencies of the updated model, the percentage error and the MAC coefficients are shown. It is possible to note that the model natural frequencies are very close to the experimental ones and the correlation (MAC) between mode shapes shows very good agreement for the bending mode shapes (excellent agreement for the first two modes), and only for the torsional mode a low correlation between modes has been obtained, as expected considering the position of the accelerometers (see Fig. 3). In fact, the present

Table 2
Comparison of the experimental data with the updated model.

	Experimental [Hz]	Model [Hz]	MAC
Mode 1	2.301	2.331	0.992
Mode 2	2.429	2.339	0.966
Mode 3	4.187	4.473	0.061
Mode 4	4.599	5.503	0.702
Mode 5	5.017	5.504	0.748

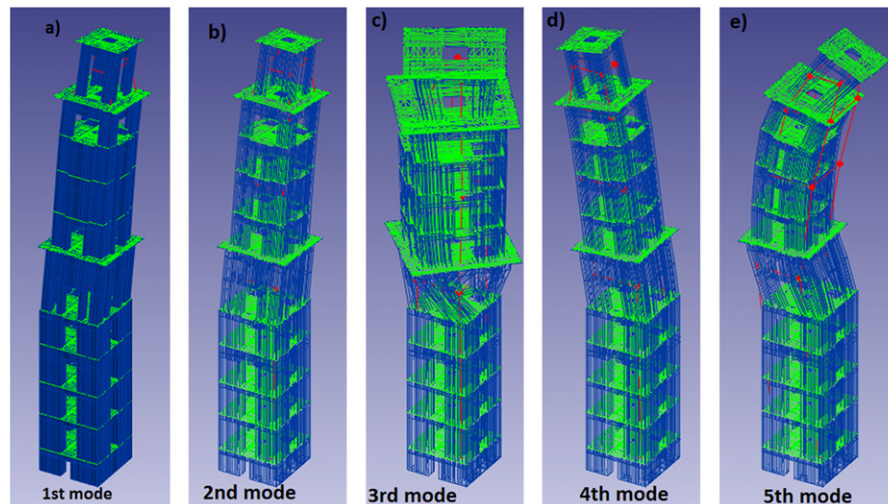


Fig. 12. Comparison between the first five experimental identified modes and numerical modes. (For interpretation of the references to colour in this figure legend, the reader is referred to the web version of this article.)

Table 3

Updating of the value of E and ρ for the different 11 zones of the model.

Zone	Starting value of $E \cdot 10^{11} \text{ N/m}^2$	Final value of $E \cdot 10^{11} \text{ N/m}^2$	Percentage difference for E	Starting value of $\rho \cdot 10^3 \text{ kg/m}^3$	Final value of $\rho \cdot 10^3 \text{ kg/m}^3$	Percentage difference for ρ
1	2.2	3.3	50	2.2	2.199	−0.0002
2	2.2	3.3	50	2.2	2.199	−0.0002
3	2.2	3.3	50	2.2	2.197	−0.001
4	2.2	3.3	50	2.2	2.191	−0.004
5	2.2	3.3	50	2.2	2.187	−0.007
6	2.2	1.38	−37	2.2	3.3	50
7	2.2	3.3	50	2.2	3.3	50
8	2.2	3.3	50	2.2	3.3	50
9	2.2	1.1	−50	2.2	1.1	−50
10	2.2	1.1	−50	2.2	1.1	−50
11	2.2	1.1	−50	2.2	1.1	−50

analysis has been carried out with an under-size number of accelerometers, that does not permit a satisfactory reconstruction of the torsional mode relative to the displacements of the 7th and 9th floors (the accelerations have been measured only along two directions). Moreover, in Fig. 12 the comparison between the first five experimental (red continuous lines) and numerical mode shapes are shown: the overlapping is evident and the correlation is demonstrated for all the bending modes, besides. Observing the torsional mode, it is evident that the experimental and the theoretical ones are similar, nevertheless the low value of MAC index.

Some interesting considerations may be carried out analyzing the results of the updating process: the springs variation may be considered negligible respect to the starting value (maximum variation less than 0.1%), while the other parameters have been substantially changed, but within the maximum range of 50% of the starting values. In detail, in Table 3 the changes of the Young's modulus and densities referred to the 11 zones indicated in Fig. 9 are shown. Analyzing Table 3 it is possible to note that, except for zone 6, the trend of the Young's modulus values and the densities during the updating procedure is similar, showing a decrease in the higher floors of the tower and an increase in the lower floors respect to the starting value.

The results of the updating process for the 44 masses are shown in Table 4, considering that the masses have been counted starting from the lower floors towards the higher ones. Analyzing Table 4, it is interesting to note that the trend (last column) is really similar to the density trend of Table 3: no changes for the

first values (corresponding to zones 1–5 of Table 3 and Fig. 9), increasing for the intermediate values (zones 6–8) and decreasing for the last values (zones 9–11). This corresponding trend demonstrates a coherent updating that tries to make lighter the superior part of the tower respect to a homogeneous mass distribution in the tower.

7. Conclusions

The ambient-vibration based investigations carried out to assess the dynamical behavior of the tower of the Provincial Administration Building of Bari have been presented in this paper. Eleven consecutive ambient vibration tests were conducted for the accurate estimation of the dynamic characteristics, evaluating the statistical repeatability of the results. Moreover, a FE model with 3D elements was realized and updated considering the experimental measurements.

The following conclusions can be drawn from this study:

1. The fundamental mode of the tower, with a natural frequency of about 2.3 Hz, involves dominant bending in E/W direction (that is y-axis in the reference system introduced). The coupled motion (about 2.4 Hz) is referred to N/S direction (x-axis).
2. The second couple of bending modes are around 5 Hz and between these two couples of modes there is a torsional mode at a value a bit higher than 4 Hz. Observing the experimental measurements, the last mode is not really clear, probably due

Table 4

Updating of the value of the concentrated masses.

Progressive mass number	Starting value of $m \cdot 10^3$ kg	Final value of $m \cdot 10^3$ kg	Percentage difference for m	Progressive mass number	Starting value of $m \cdot 10^3$ kg	Final value of $m \cdot 10^3$ kg	Percentage difference for m
1	11.24	11.24	0	23	37.22	55.83	50
2	11.70	11.70	0	24	33.60	50.39	50
3	21.51	21.51	0	25	18.66	27.99	50
4	21.15	21.15	0	26	18.66	27.99	50
5	36.18	36.18	0	27	18.66	27.99	50
6	17.90	17.90	0	28	18.66	27.99	50
7	19.30	19.30	0	29	18.66	27.99	50
8	36.18	36.18	0	30	20.49	22.17	8.2
9	29.74	29.74	0	31	20.49	22.23	8.5
10	17.37	17.37	0	32	20.49	21.24	3.7
11	19.88	19.88	0	33	22.99	12.7	–44.8
12	29.74	29.74	0	34	20.13	11.96	–40.6
13	33.03	33.03	0	35	20.13	11.97	–40.5
14	17.09	17.09	0	36	22.99	12.72	–44.7
15	31.11	31.11	0	37	23.96	23.65	–1.31
16	33.30	33.30	0	38	23.96	30.87	28.8
17	57.87	57.87	0	39	23.96	30.24	26.2
18	31.01	31.01	0	40	23.96	23.27	–2.89
19	50.98	50.98	0	41	19.88	9.94	–50
20	50.51	50.51	0	42	17.01	8.5	–50
21	33.60	50.39	50	43	17.01	8.5	–50
22	37.22	55.83	50	44	19.88	9.94	–50

to the positioning of the accelerometers that, for the same instrumented floors, were not sufficient to describe the torsional vibrations. Nevertheless, the theoretical model fully clarifies the nature of the third mode.

3. A very good agreement was found between the modal estimates obtained from the two classical OMA methods, EFDD and SSI, and the recently implemented CC-SSI method, for each of the consecutive acquisition intervals.
4. The good match between measured and predicted modal parameters was reached with an updating procedure tuned with a maximum variation of $\pm 50\%$ of the initial values of the parameters (Young's modulus, density, concentrated masses and springs) which have been opportunely measured or estimated as previously explained.
5. Due to the good correlation between experimental and theoretical models, the updated model seems to be adequate to provide reliable predictions to assess the structural situation of the tower and this result is particularly important considering the highly inhomogeneous materials (stones and cyclopic concrete) that compose the tower itself.

Acknowledgments

The research was supported by Strategic Project PS060 – “Innovative structures and Advanced Material Experimentation” – S.I.S.M.A. – Apulia Region.

References

- [1] Sepe V, Speranza E, Viskovic A. A method for large-scale vulnerability assessment of historic towers. *Struct Control Health Monit* 2008;15(3):389–415.
- [2] Valluzzi MR, da Porto F, Modena C. Structural investigation and strengthening of the Civic Tower in Vicenza. *Proc of Structural Faults and Repairs*, London UK: 2003.
- [3] Ivorra S, Pallarés FJ. Dynamic investigations on a masonry bell tower. *Eng Struct* 2006;28(5):660–7.
- [4] Gentile C, Saisi A. Ambient vibration testing of historic masonry towers for structural identification and damage assessment. *Constr Build Mater* 2007;21(6):1311–21.
- [5] Julio ENBS, Da Silva Rebelo CA, Dias–Da–Costa D. Structural assessment of the tower of the University of Coimbra by modal identification. *Eng Struct* 2008;30:3648–77.
- [6] Lepidi M, Gattulli V, Foti D. Swinging-bell resonances and their cancellation identified by dynamical testing in a modern bell tower. *Eng Struct*, Elsevier 2009; 31 (7): 1486–1500.
- [7] Ramos LF, Marques L, Lourenco PB, de Roeck G, Campo-Costa A, Roque J. Monitoring historical masonry structures with operational modal analysis: Two case studies. *Mech Syst Signal Process* 2010;24:1291–305.
- [8] Bayraktar A, Sevim B, Altunisik AC, Türker T. Earthquake analysis of reinforced concrete minarets using ambient vibration tests results. *Struct Des Tall Spec Build* 2008;19:257–73, doi:10.1002/tal.464.
- [9] Jacobsen NJ, Thorhauge O. Data acquisition systems for Operational Modal Analysis. *Proc 3rd IOMAC*, 215–22, Porto Novo (Ancona) 2009.
- [10] Masjedjan MH, Keshmiri M. A review on operational modal analysis researches: classification of methods and applications. *Proc 3rd IOMAC*, 707–18, Starrylink, Brescia 2009.
- [11] Brincker R, Zhang L, Andersen P. Modal identification of output-only systems using frequency domain decomposition. *Smart Mater Struct* 2001;10:441–5.
- [12] Peeters B, De Roeck G. Stochastic system identification for operational modal analysis: a review. *J Dyn Syst Meas Control* 2001;123(4):659–67.
- [13] Foti D, Diaferio M, Mongelli M, Giannocaro NI, Andersen P. Operational modal analysis of a historical tower in bari, *Civil Engineering Topics*, Vol. 4, isbn 978-1-4419-9315-1. Conf Proc Soc Experimental Mechanics Series, “IMAC XXIX” 2011; 7: p. 335–42. doi:10.1007/978-1-4419-9316-8_31, 31 January–3 February 2011, Jacksonville, Florida, USA.
- [14] ARTeMIS Extractor Pro software. Issued by Structural Vibration Solutions ApS. NOV1 Science Park, Niels Jernes Vej 10, DK 9220 Aalborg East, Denmark; 2009.
- [15] SAP2000 Advanced 11.0.0. Computers and Structures, Inc. 1978–2006. Berkeley, CA.
- [16] UNI 6556:1976. Prove sui calcestruzzi. Determinazione del modulo elastico secante a compressione. Ente Nazionale Italiano di Unificazione.
- [17] Dynamic Design Solution NV (DDS). Fem Tools Model Updating Theoretical Manual. Dynamic Design Solution NV (DDS) Interleuvenlaan 64, 3001, Leuven, Belgium; 2008.
- [18] Friswell MI, Mottershead JE. Finite element model updating in structural dynamics. The Netherlands, Dordrecht: Kluwer Academic; 1995.
- [19] FEM Model Updating 3.3 theoretical manual Vers. 3.3., Dynamic Design Solutions NV (DDS), June 2008.